

Exploration of Galactic γ -Ray Supernova Remnants

TIAN Wenwu^{*}, ZHANG Jianli

National Astronomical Observatories, CAS, Beijing, 100012

New generational very-high-energy telescope arrays have been detecting more than 120 TeV γ -ray sources. Multi-wavelength observations on these Gamma-ray sources have proven to be robust in shedding light on their nature. The coming radio telescope arrays like ASKAP and FAST may find more faint (extended) radio sources due to their better sensitivities and resolutions, might identify more previously un-identified γ -ray sources and set many new targets for future deep surveys by very-high-energy ground-based telescopes like LHAASO. We in the paper summarize a list of known Galactic γ -ray Supernova Remnants (SNRs) with or without radio emissions so far, which includes some SNRs deserving top priority for future multi-wavelength observations.

Supernova remnants, gamma-ray sources, Cosmic rays

PACS number(s): 98.38.Mz, 98.70.Rz, 98.70.Sa

1. Background

Astrophysical shock waves have been considered as efficient accelerators of Cosmic Rays (CRs, mainly composed of nuclei, protons and electrons) since the 1980's [1]. Based on the inferred Galactic CR energy density ($1-2 \text{ eV/ cm}^3$) and the inferred time ($\sim 6 \times 10^6$ yrs) that an average cosmic ray stays in the Galaxy, the Galactic CRs have a total power of $\sim 10^{41}$ erg /s. By comparison with the supernova energy and rates (their average explosion energy of $\sim 10^{51}$ erg and an inferred Galactic supernova rate of $\sim 2 - 3$ per century), Galactic Supernova Remnant (SNR) shocks accelerating charged particles in the interstellar medium (ISM) and circum-stellar medium (CSM) are able to produce most of the Galactic cosmic rays up to 10^{15} eV . As a key issue to explore the origin of the CSs, we need first understand the relative efficiency of acceleration of protons versus electrons as well as the maximum energies obtained.

CRs are mainly composed of charged particles which are deflected in the magnetic fields, so direct observations on the charged particles carry no information on their origin. However, observations of Gamma-ray photons as small components of the CRs ($<1\%$) play a key role in this issue due to two reasons: Gamma-rays have straight-line propagation; Gamma-rays may be produced by relativistic particles' interactions.

New generational very-high-energy telescope arrays have detected more than 120 TeV γ -ray sources in the Universe in recent years. Seeking low-energy band counterparts of TeV sources plays a key role in shedding light on the nature of the TeV sources. Two major γ -ray generators have been identified now, i.e. young shell-type SNRs and pulsar wind nebulae [2,3]. There are also other possible candidates as counterparts to some unidentified TeV sources[4, 5,6].

^{*} Corresponding author (email:tw@bao.ac.cn)

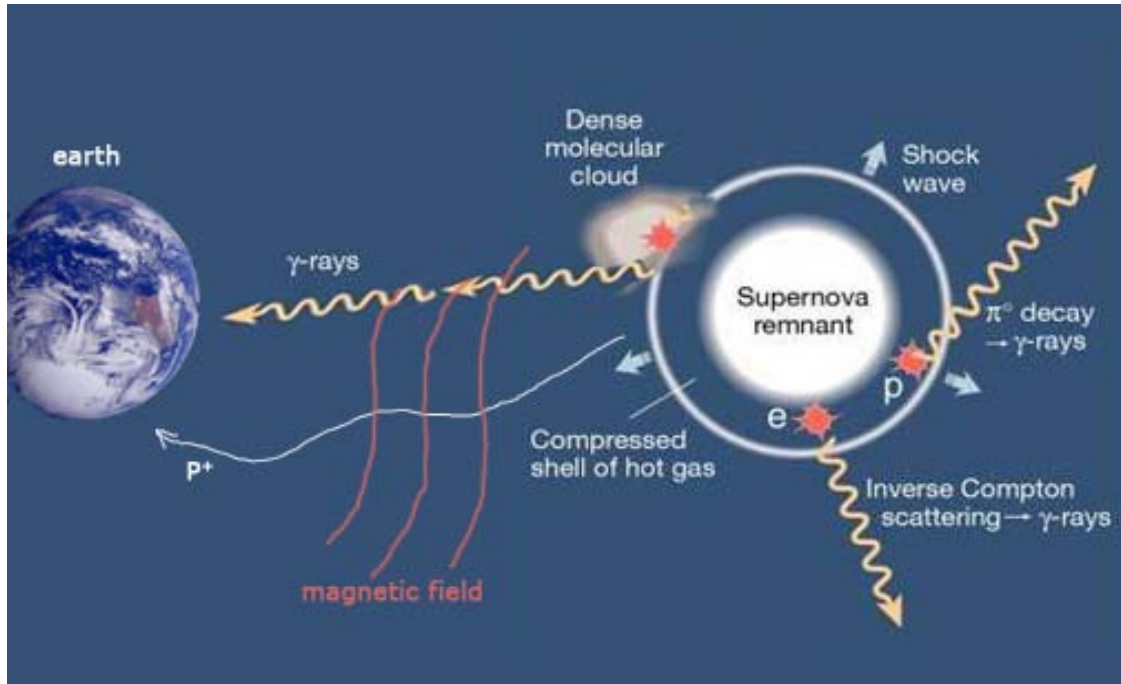


Fig. 1 diagrams that γ -rays from cosmic ray sources are straight-line transportation while charged particles are deflected in ISM magnetic fields on their travel from the origin to the Earth. Two main γ -ray emission mechanisms here are: hadronic origin and leptonic origin (for details please refer to the text). Credits go to Mr. SU Hongquan for helping produce Figure 1 which in turn benefits from Dr. Aharonian's paper (<http://www.nature.com/nature/journal/v416/n6883/full/416797a.html>).

With the advent of new general X-ray and γ -ray observatories (e.g., XMM-NEWTON, Chandra, HESS, Fermi etc), recent observations have shown that SNR shocks are able to accelerate particles to TeV energies[7,2,8]. Theoretical exploration has revealed that two primary TeV photon emission mechanisms play major roles in the processes, i.e., the decay of neutral pions (π^0) by p-p interactions and the inverse-Compton scattering of electrons on ambient photons. These particles may or may not immediately escape the acceleration and emission sites due to the presence of magnetic fields in SNR, which depends on the energy threshold of particles. Part of the charged particles may be detected after they escape to the interstellar space from the accelerating sites when the MHD disturbance which constrains the particles gets decreased. However, it is still extremely difficult for us to trace their accelerating sites by detecting them because Galactic magnetic fields have changed their directions of transmission. However, the TeV photons tell us different story because they escape directly and transmit in a straight-line way, which makes it possible to find the sites of these processes.

Observations in the radio, X-ray and γ -ray wavebands are so far the best way to access non-thermal acceleration processes in SNR. Although studying γ -rays emissions may point to the sites of the particle acceleration, the particles are either hadrons or leptons due to existing two main mechanisms. So far, we might have detected the two classes of TeV γ -ray photons from SNR, but we cannot claim that we have solved the CRs' origin issue before we may clearly distinguish them.

Studying evolved SNRs of older than 10^3 yr seems bring new hopes because evolved SNRs have very different characteristics comparing to young SNRs. [4] have revealed that the γ - and X-ray emissions in an evolved SNR are expected to be dominated by the decay of neutral pions and by the synchrotron radiation of secondary electrons from charged pion decay, respectively.. So detecting both γ - and X-ray emissions from many faint radio SNRs might provide key evidence that Galactic CRs originates from SNRs' accelerating charged particles.

Recently, we have given evidence of CRs originating from old SNR using multi-wave observations. Based on a new distance-measurement method, [9] provided observational evidence supporting that the old SNR W41 encounters a GMC to emit TeV γ -rays (HESS J1834-087). In this case, the CR protons could diffuse only partway into the cloud, resulting in p-p to π^0 decay TeV γ -rays, so TeV γ -rays in W41 primarily have hadronic origin. Further, [10] discovered a new faint SNR G353.6-0.7 with age of 27000 yrs, whose radio and X-ray morphologies closely match the outline of HESS J1731-347, one previously unidentified extended TeV source. Deep research using new results from XMM-Newton and SUZAKU X-ray observations, and Delinha CO observations demonstrated that G353.6-0.7 may be coincident with CO clouds. Based on the probable association between the X-ray and gamma-ray emissions and likely association between the CO cloud and the SNR, [8] argued that the extended TeV emission originates from the interaction between the SNR shock and the adjacent CO clouds.

Our study has shown that it is highly likely that evolved SNRs, as well as young SNRs, play a key role in proving that SNRs are the source of the Galactic CRs. Especially, almost half of the detected Galactic TeV γ -rays sources so far have no low energy-band's counterparts. For upcoming very-high-energy telescope surveys, more such unidentified TeV sources will be found (e.g. CTA, LHAASO) . To identify the unidentified TeV sources becomes increasingly important. However, it is difficult to do this by using current radio and X-ray instruments as a result of their limited sensitivity, if the TeV sources are faint SNRs. In fact, there is a discrepancy between the number of known SNRs (276) and the number predicted by theory (above 2000 Galactic SNRs). This has been considered the result of selection effects in current sensitivity-limited surveys, which favor the discovery of the brighter remnants (e.g. [11]). Survey data from observations that combine high sensitivity and resolution with low radio frequencies are becoming the rich modern hunting-grounds for new SNRs. Some new SNRs have been discovered from the 90 cm Very Large Array survey of the inner Galaxy [12], the Canadian Galactic Plane Survey (CGPS) of the outer Galaxy[13,14], the Southern Galactic Plane Survey [10], and a Sino-German 6 cm polarization survey of the Galactic plane[15] .

2. Current Statistics Results

New general space and ground-based high-energy telescopes have detected many gamma-ray sources. Most Galactic gamma-ray sources are probably associated with SNRs/PWNs. Table 1 shows all Galactic TeV SNRs/PWNs (Table 1) and Table 2 is the Galactic GeV SNRs/PWNs and unidentified TeV sources, based on all accessible observations and references so far. We focus on

the GeV/TeV sources with radio emissions. We have only selected the SNRs with GeV/TeV emission in the catalog compiled by Ferrand & Safi-Harb[16] (see <http://www.physics.Umanitoba.ca/snr/SNRcat>), which includes all the high energy SNRs in the Galaxy. We have added the TeV sources not appearing in Ferrand & Safi-Harb's catalog but appearing in the TeV catalog (see <http://tevcat.uchicago.edu>). Some TeV sources have not been identified by other wave band observations so far. We have also given/calculated fluxes of the GeV/TeV SNRs with the unit of Crab. In addition, we have made notes if a SNR is in the LHAASO's field of view as a bonus for the LHAASO design. In the tables, the second column is the "SNR ID Gal. name" which uniquely identifies the object (with its Galactic coordinates). The columns "RA(2000)" and "Dec(2000)" give the location (Right Ascension and Declination of the J2000). The column "LHAASO" shows whether the SNR/PWN is in the field of view of LHAASO. The sixth column "name (Gamma-ray)" are gamma-ray source names. The seventh column is the morphology type. Columns eight and nine are the age and distance. column twelve "SNR/MC" shows if there exists an interaction between SNR shock with adjacent molecular clouds. Symbol "?" hints an uncertainty in TeV sources' classification and association relationship.

2.1. Current Catalogue of Gamma-Ray/SNR Associations: GeV/TeV Galactic SNR

Table 1 lists 61 TeV gamma ray sources, which are likely identified as SNRs/PWNe. Most of them are discovered by H.E.S.S., 21 cases of which are in LHAASO field of view. 28 cases of TeV sources have likely shell structures (20 are considered certain, and 8 have not been identified). 32 of TeV sources have been considered as PWN (28 are certain, and 4 are possible). 28 cases are composite (11 are confirmed, and 17 are possible). Association with a molecular cloud has been reported in 28 cases, and 4 cases are considered unlikely. Most of them with measured distances are nearby, i.e. 32 of 52 cases have distances less than 6 kpc. Many SNRs are very young, i.e. 17 of 39 cases with known ages have ages less than 3 k years.

Table 1: TeV Galactic SNRs/PWNe which have radio or X-ray counterparts

	SNR ID Gal. name	RA (2000)	Dec (2000)	LHAA SO	Name (Gamma- ray)	Type	Age (kyr)	Distance (kpc)	Radio size	Gamma -Flux (Crab Units)	SNR/ MC	Refs
1	G0.0+0.0(SGR A East)	17h 45m 44s	-29° 00' 00"	N	HESS J1745-290(GT)	S?	8	8.5	2.5'-3.5'	0.05(≥ 0.165 TeV)(H,V,C,MA,F)	Y	17, 18, 19, 20, 21, 22, 23, 24, 25, 26, 27
2	G0.9+0.1	17h 47m 21s	-28° 09' 00"	N	HESS J1747-281(T)	C PWN	1.9(S), 5(P)	10(S),13(P)	8'	0.02(≥ 0.2 TeV)(H)		17, 28
3	G5.7-0.1?	17h 58m 49s	-24° 03' 00"	N	HESS J1800-240C(T)		35-45		9' - 12'	0.01(0.3-5TeV)(H)	Y	17, 29
4	G5.9-0.37	18h 00m 26.4s	-24° 02' 20.4"	N	HESS J1800-240B(GT)	S? C?	35-45			0.02(0.3-5TeV)(H,F)		17, 29
5	G6.14-0.63	18h 01m 57.8s	-23° 57' 43.2"	N	HESS J1800-240A(GT)	S? C?	35-45			0.02(0.3-5TeV)(H,F)		17, 29
6	G6.4-0.1(W28)	18h 00m 30s	-23° 26' 00"	N	(GT)	C	35-45(S)	1.8 - 1.9(S)	48'	(H)	Y	17, 29
7	G6.5-0.4	18h 02m 11s	-23° 34' 00"	N	HESS J1801-233(T)	S			18'	0.02(0.3-5TeV)(H)		17, 29
8	G8.7-0.1(W30)	18h 05m 30s	-21° 26' 00"	N	HESS J1804-216(GT)	S? PWN	10-50	4(S,P)	45'	0.25(≥ 0.2 TeV)(H,C,F)	Y	17, 30
9	G11.2-0.3	18h 11m 27s	-19° 25' 00"	N	HESS J1809-193(T)	C	≤ 2 (S), 24(P)	≥ 5 (S) 5(P)	4'	0.14(≥ 0.25 TeV)(H)	N	
10	G12.8-0.0(W33)	18h 13m 37s	-17° 49' 00"	N	HESS J1813-178(T)	C? PWN	1.2(S), 5(P)	4.7(P)	3'	0.06(≥ 0.2 TeV)(H,MA)	N	
11	G15.4+0.1	18h 18m 02s	-15° 27' 00"	N	HESS J1818-154(T)	S?			14'-15'	0.018(≥ 1 TeV)(H)	5	31

12	G18.0-0.7	18h 25m 41s	-13° 50' 20"	N	HESS J1825-137(GT)	PWN		4(P)		0.17(\geq 0.2TeV)(H,F)		32, 33, 34
13	G21.5-0.9	18h 33m 33s	-10° 35' 00"	N	HESS J1833-105(T)	C PWN	0.7-1.07(S), 4.8(P)	4.7(S,P)	4'	0.02(\geq 0.2TeV)(H)	Y?	17, 35
14	G22.7-0.2	18h 32m 46.83s	-09° 21' 54.5"	Y	HESS J1832-093(T)	S?			26'	0.007(\geq 1TeV)(H)	Y?	36
15	G23.3-0.3(W41)	18h 34m 45s	-08° 48' 00"	Y	HESS J1834-087(GT)	S? PWN ?	100(S)	3.9-4.5(S)	27'	0.08(\geq 0.2TeV)(H,MA,F)	Y?	17, 37, 38,
16	G25.5+0.0	18h 37m 38.4h	-06° 57' 00"	Y	HESS J1837-069(T)	PWN ?				0.132(\geq 0.2TeV)(H)		32
17	G29.7-0.3(Kes 75)	18h 46m 25s	-02° 59' 00"	Y	HESS J1846-029(T)	C PWN	0.9-4.3(S), 0.725(P)	5.1-7.5(Tian)	3'	0.02(\geq 0.25TeV)(H)	Y	17, 39
18	G32.8-0.1(Kes 78)	18h 51m 25s	-00° 08' 00"	Y	HESS J1852-000(T)	S?		4.8(S)	17'	?(H)	Y	17, 40, 41
19	G35.6-0.4 ?	18h 54m 53s	02° 33' 25"	Y	HESS J1858+020(T)	S	30(S), 160(P)	3.7-10.5(S), 8(P)	11'-15'	0.018(0.5-80TeV)(H)		42, 43
20	G40.5-0.5	19h 07m 10s	06° 31' 00"	Y	HESS J1908+063,MGR O 1908+06(GT)	S	20(P)	3.2(P)	22'	0.17(\geq 1TeV)(H,V,MI,A,F)	Y?	44, 45
21	G43.3-0.2(W49 B)	19h 11m 08s	09° 06' 00"	Y	HESS J1911+090(GT)	C	1-4(S)	8 – 11(S)	3' - 4'	0.005(\geq 0.26TeV)(H,F)	Y	37, 46, 47
22	G49.2-0.7 (W51)	19h 23m 50s	14° 06' 00"	Y	HESS J1923+141(GT)	C? PWN	10(S)	5.5 – 6(S)	30'	0.003(\geq 1TeV)(H,MA,F)	Y	17, 48, 49, 50, 51

23	G54.1+0.3	19h 30m 31s	18° 52' 00"	Y	(T)	PWN	2.5-3.3(S), 2.9(P)	5.6-7.2(S),5(P)	1.5'	0.025(\geq 1TeV)(V)	Y?	
24	G65.1+0.6	19h 54m 40s	28° 35' 00"	Y	0FGL J1954.4+2838(GT)	S	4-14	9.2(S)	50'-90'	0.23(\approx 35TeV)(MIF)		
25	G74.9+1.2(CTB 87)	20h 16m 02s	37° 12' 00"	Y	VER J2016+372(GT)	C? PWN		6.1-12(S)	6' - 8'	0.01(\geq 1TeV)(V,A)	Y?	52, 53, 54
26	G75.2+0.1(Cisne)	20h18m 35.03s	36°50'00"	Y	MGRO J2019+37(T)	PWN ?		\geq 10(S),4(P)		0.67(\approx 35TeV)(MI)		52, 55, 53, 56
27	G78.2+2.1(gammaCygni)	20h 20m 50s	40° 26' 00"	Y	VER J2019+407(GT)	S	6.6(S)	1.5(S)	60'	?(V,F)	Y?	17, 57, 58, 59, 60
28	G106.3+2.7(Boomerang)	22h 27m 30s	60° 50' 00"	Y	2FGL J2229.0+6114(GT)	C? PWN	10(P)	0.8(S),3(P)	24' - 60'	0.05 (\geq 1TeV)(V,MI,F)	Y?	17, 59, 61
29	G111.7-2.1(Cas A)	23h 23m 26s	58° 48' 00"	Y	2FGL J2323.4+5849(GT)	S	0.316 -0.352(S)	3.3 - 3.7(S)	5'	0.03(\geq 1TeV)(V,MA,F)	Y?	17, 62
30	G119.5+10.2	00h 06m 40s	72° 45' 00"	N	CTA 1(GT)	S PWN	13-17	1.4(S)	90'	0.04(\geq 1TeV)(V,F)		17, 63, 1, 64
31	G120.1+1.4	00h 25m 18s	64° 09' 00"	Y	Tycho(GT)	S	0.440	2.5-5(S)	8'	0.009 (MA,F)	Y?	57, 58, 65, 66, 67, 68, 69, 70
32	G184.6-5.8	05h 34m 31s	22° 01' 00"	Y	Crab(GT)	C? PWN	0.958	1.5-2.5(S), 2(P)	5' - 7'	1(H,V,MA,MI,A,F)	N	17, 71, 72, 73
33	G189.1+3.0(IC443)	06h 17m 00s	22° 34' 00"	Y	MAGIC J0616+225(GT)	C PWN	30(S), P)	0.7 - 2(S)	45'	0.03 (V,MA,MI,F)	Y	17, 74
34	G195.1+4.3	06h 32m 28s	17° 22' 00"	Y	Geminga (GT)	C? PWN		0.25(P)		0.23(35TeV)(MI,F)		35

35	G205.5+0.5(Monoceros)	06h 39m 00s	06° 30' 00"	Y	HESS J0632+057(GT)	S	30-150	0.8 - 1.6(S)	220'	0.03(\geq 0.4TeV)(H,MA,V,F)	Y?	17
36	G263.9-3.3(Vela X)	08h 34m 00s	-45° 50' 00"	N	HESS J0835-455(GT)	C PWN		0.25-0.3(S), 0.29(P)	255'	0.75(\geq 0.45TeV)(H,F)	Y?	17, 35, 75
37	G266.2-1.2(Vela Jr.,RX J0852.0-4622)	08h 52m 00s	-46° 20' 00"	N	HESS J0852-463(GT)	S	0.6-4(S)	0.2 - 2.4(S)	120'	1(0.3-20TeV)(H,C,F)	?	17, 76, 77, 56
38	G284.3-1.8(MSH 10-53)	10h 18m 15s	-59° 00' 00"	N	HESS J1018-589(GT)	S PWN	10(S)	2.9(S),3(P)	24'	?(H,F)	Y	17, 78
39	G292.2-0.5	11h 19m 20s	-61° 28' 00"	N	HESS J1119-614(T)	S PWN	\leq 1.7(S) 1.6(P)	8-8.8(S), 1.6(P)	15'-20'	0.04(0.5-10TeV)(H)		17
40	G304.1-0.2	13h 03m 0.4s	-63 11 55	N	HESS J1303-631(T)	C? PWN		7(P)		0.17(\geq 0.38TeV)(H)		79, 80
41	G309.9-2.5	13h 56m 00s	-64° 30' 00"	N	HESS J1356-645(GT)	C? PWN		2.5(P)		0.11(1-10TeV)(H,F)		81, 82, 83
42	G313.3+0.1(Rabbit)	14h 18m 04s	-60° 58' 31"	N	HESS J1418-609(GT)	C? PWN		5.6		0.06(\geq 0.3TeV)(H,F)		44
43	G313.6+0.3(Ko-okaburra)	14h 20m 09s	-60° 45' 36"	N	HESS J1420-607(GT)	C? PWN	13(P)	5.6(P)		0.07(\geq 0.3TeV)(H,F)		44
44	G315.4-2.3(RCW 86)	14h 43m 00s	-62° 30' 00"	N	HESS J1442-624(T)	S	2-10(S)	2.4 - 3.2(S)	42'	0.1(\geq 0.48TeV)(H)	?	17, 84, 85
45	G318.2+0.1	14h 54m 50s	-59° 04' 00"	N	HESS J1457-593(T)	S		3.5-9.2(S)	35'-40'	?(H)		17, 86

46	G320.4-1.2(RCW 89,MSH 15-52)	15h 14m 30s	-59° 08' 00"	N	HESS J1514-591(GT)	C PWN	1.9(S),1.7(P)	3.8-6.6(S), 5(P)	35'	0.15(≥ 0.28 TeV)(H,C,F)		17, 32, 44
47	G327.1-1.1	15h 54m 25s	-55° 09' 00"	N	(T)	C	11(S)	9(S)	18'	0.015(1-10TeV)(H)		17, 87
48	G327.6+14.6(SN 1006)	15h 02m 50s	-41° 56' 00"	N	HESS J1502-421/HESS J1504-418(T)	S	1.006	2.1 - 2.3(S)	30'	0.01 (≥ 1 TeV)(H)	N	17
49	G332.5-0.3	16h 16m 24s	-50° 53' 60"	N	HESS J1616-508(T)	C? PWN		6.5(P)		0.19(≥ 0.2 TeV)(H)		79, 80
50	G335.2+0.1	16h 27m 45s	-48° 47' 00"	N	HESS J1626-490(GT)	S			21'	0.16(0.6-50TeV)(H)		17, 88
51	G337.2+0.1	16h 35m 55s	-47° 20' 00"	N	HESS J1634-472(GT)	C? PWN ?	1.5(S)	14(S)	2' - 3'	0.12(≥ 0.2 TeV)(H)		17
52	G338.3-0.0	16h 41m 00s	-46° 34' 00"	N	HESS J1640-465(GT)	C? PWN	4.5-8.2(S)	8 - 13(S)	8'	0.09(≥ 0.2 TeV)(H,F)		17
53	G343.1-2.3	17h 08m 00s	-44° 16' 00"	N	HESS J1708-443(T)	C? PWN	17.5(P)	2(P)	32'	0.17(1-10TeV)(H,C)		17, 89
54	G344.7-0.1	17h 03m 51s	-41° 42' 00"	N	HESS J1702-420(T)	C?		14(S),5(P)	10'	0.07(≥ 0.2)(H)	Y?	17, 90, 91, 92
55	G345.7-0.2	17h 07m 20s	-40° 53' 00"	N	HESS J1708-410(T)	S			6'	0.04(≥ 0.2 TeV)(H)		17, 79, 80
56	G347.3-0.5	17h 13m 50s	-39° 45' 00"	N	RX J1713.7-3946(GT)	S?	1-10(S)	1 - 6(S)	55'-65'	0.66(≥ 1 TeV)(H,C,F)	Y	17, 56, 93, 94, 95, 96
57	G348.5+0.1(CTB 37A)	17h 14m 06s	-38° 32' 00"	N	HESS J1714-385(GT)	S PWN	1-3(S)	6.3-9.59(S)	15'	0.03(≥ 1 TeV)(H,F)	Y	17, 97, 98

58	G348.7 +0.3(CT B 37B)	17h 13m 55s	-38° 11' 00"	N	HESS J1713-38 1(T)	S	0.35– 3.15(S),0.9 5(P)	13.2 (S)	55' - 65'	0.018(\geq 0.2TeV) (H)	Y	17, 97, 99
59	G348.9- 0.4	17h 18m 07s	-38° 33' 00"	N	HESS J1718-38 5(T)	C? PWN		4(P)		0.02(1- 10TeV) (H)		
60	G353.6- 0.7	17h 32m 00s	-34° 44' 00"	N	HESS J1731-34 7(T)	S	27(S)	2.4 - 4 (S)	30'	0.16(1- 10TeV) (H)	Y?	17, 100
61	G359.1- 0.5	17h 45m 30s	-29° 57' 00"	N	HESS J1745-30 3(T)	C	20–5 0		24'	0.05(\geq 0 .2TeV)(H)	Y	17, 79, 80, 101, 102

LHAASO: “N” means the source is not in the field of view of LHAASO. “Y” means it should be detected by LHAASO.

Name (Gamma-ray): GT: emissions are both measured by Fermi in GeV and other ground-based telescopes in TeV; G: emission is measured only by Fermi in GeV; T: emission is measured only by ground-based telescope(s) in TeV.

Type: Composite=C, Shell = S, Pulsar Wind Nebula = PWN.

Age/Distance: Shell=S, Pulsar=P. Distances of CTB 37A/B are from Tian & Leahy (2012, MNRAS, online earlier version).

Gamma-Flux (Crab Units): H=HESS, V=VERITAS, MA=MAGIC, C=CANGAROO, MI=Milagro, A=ARGO-YBJ, F=FERMI, HE=HEGRA, W=Whipple. Fermi measurements are in the energy range of 1-100GeV. Crab Units: Crab flux[错误! 未定义书签。]: differential: $3.45E-11*(E/1TeV)^{-2.63} \text{ cm}^{-2}\text{s}^{-1}\text{TeV}^{-1}$.

SNR/Molecular Cloud: “Y” = Yes, “Y?” =likely, “N” = unlikely.

The data used here are mostly from website catalogs: <http://www.physics.umanitoba.ca/snr/SNRcat>, <http://tevcat.uchicago.edu> and Caprioli D. [103].

The SNR/MC interactions listed in column 12 are gotten from Ferrand & Safi-Harb’s catalog, also referencing the paper of Jiang B. et al. [104].

2.2 Unidentified GeV-TeV Galactic Sources

There are 61 GeV-TeV gamma ray sources in this list: 19 are unidentified TeV objects, and 42 are identified as SNRs discovered by Fermi Gamma-ray LAT. In 30 cases, the object has shell: 25 are considered certain, 5 have not been confirmed. 8 cases have been considered as PWN: 6 are certain, and 2 are possible. 12 cases are composite: 7 are confirmed, and 5 are possible. Association with a molecular cloud has been reported in 12 cases in GeV cases.

Table 2: Galactic GeV SNRs/PWN and no X-ray or radio counterpart TeV sources

	SNR ID Gal. name	RA (2000)	Dec (2000)	LHAA SO	Name (Gamma-ray)	Type	Age (kyr)	Distance (kpc)	Radio size	Gamma-Flux (Crab Units)	SNR/MC	Refs
1	G5.4-1.2?(Milne 56)	18h 02m 10s	-24° 54' 00"	N	2FGL J1802.3-2445 c(G)	C?		4.3-4.5(S), 5(P)	35'	0.024(F)	Y	17
2	G11.4-0.1	18h 10m 47s	-19° 05' 00"	N	2FGL J1811.1-1905 c(G)	S?			8'	0.017(F)		17
3	G20.0-0.2	18h 28m 07s	-11° 35' 00"	N	2FGL J1828.3-1124 c(G)	C PWN?			10'	0.024(F)		17
4	G21.85-0.11	18h 31m 25s	-09° 54' 00"	Y	HESS J1831-098(T)	PWN				0.04(\geq 1TeV)(H)		105
5	G24.7+0.6	18h 34m 10s	-07° 05' 00"	Y	2FGL J1834.7-0705 c(G)	C? PWN?			15'-30'	0.048(F)		17
6	G26.8-0.2	18h 40m 55s	-05° 33' 00"	Y	HESS J1841-055(T)					0.37(0.54-80TeV). (H)		79, 80
7	G27.4+0.0(Kes 73)	18h 41m 19s	-04° 56' 00"	Y	2FGL J1841.2-0459 c(G)	S	1.1-1.5(S), 4.3(P)	7.5-9.1(S)	4'	0.055(F)		17
8	G27.8+0.6	18h 39m 50s	-04° 24' 00"	Y	2FGL J1840.3-0413 c(G)	C			30'-50'	0.032(F)		17
9	G28.8+1.5	18h 39m 00s	-02° 55' 00"	Y	2FGL J1839.7-0334 c(G)	S?			100'	0.014(F)		17
10	G29.3+0.51	18h 43m 00s	-03° 00' 00"	Y	HESS J1843-033(T)					?(H)		
11	G31.9+0.0	18h 49m 25s	-00° 55' 00"	Y	2FGL J1849.3-0055 (G)	S	3.7-4.4(S)	\geq 7.2(S)	5' - 7'	0.04 ₁₁ (F)	Y	17
12	G32.4+0.1	18h 50m 05s	-00° 25' 00"	Y	2FGL J1850.7-0014	S			6'	0.023(F)		17

					c(G)							
13	G32.6 4+0.5 3(IGR J1849 0-000 0)	18h49m 01.63s	-00° 01' 17.2"	Y	HESS J1849-000(T)	PWN		7			0.015(≥ 0 .35TeV)(H)	
14	G33.6 +0.1(Kes 79)	18h 52m 48s	00° 41' 00"	Y	2FGL J1852.7+0047 c(G)	S	3-15(S)	7.1(S)	10'	0.01(F)	Y?	17
15	G34.7 -0.4(W44, 3C39 2)	18h 56m 00s	01° 22' 00"	Y	2FGL J1855.9+0121 e(G)	C PWN	\geq 10(S), 20(P)	3(S,P)	27'-3 5'	0.436(F)	Y	17, 106
16	G35.9 6-0.06	18h 57m 11s	02° 40' 00"	Y	HESS J1857+026(T)					0.21(0.6- 80TeV)		49, 79, 80, 107
17	G44.3 9-.07	19h 12m 49s	10° 09' 06"	Y	HESS J1912+101(T)	PWN ?				0.09 (1-10TeV)(H)		
18	G45.7 -0.4	19h 16m 25s	11° 09' 00"	Y	2FGL J1916.1+110 6(G)	S			22'	0.007(F)		17
19	G54.4 -0.3(HC40)	19h 33m 20s	18° 56' 00"	Y	2FGL J1932.1+191 3(G)	S			40'	0.042(F)	Y	17
20	G59.2 -4.7(B lack Wido w)	19h 59m 35. 8s	20° 47' 28"	Y	2FGL J1959.5+204 7 (G)	C? PWN		2.5(P)		0.015(F)		17, 108
21	G65.8 5-0.23	19h 58m 07.61s	20° 48' 11.9"	Y	0FGL J1958.1+284 8	PWN				0.21(Mi)		
22	G74.0 -8.5(C ygnus Loop)	20h 51m 00s	30° 40' 00"	Y	2FGL J2051.0+304 0e(G)	S	14(S)	0.4-0.5(S)	160'- 230'	0.062(F)	Y?	17

23	G76.9 +1.0	20h 22m 20s	38° 43' 00"	Y	2FGL J2022.8+3843 c(G)	C?	9(P)	8(S)	9'	0.013(F)		17, 109
24	G79.7 2+1.2 6	20h 29m 38.4s	41° 11' 24"	Y	MGRO J2031+41(T)					0.39(=35 TeV)(MI ,A)		45, 52, 55, 110
25	G80.2 5+1.0 7	20h 32m 07s	41° 30' 30"	Y	TeV J2032+4130(T)					0.03(=35 TeV)(HE ,W,MI,A)		52, 55, 110
26	G89.0 +4.7(HB21)	20h 45m 00s	50° 35' 00"	Y	2FGL J2041.5+5003 , J2043.3+5105 , J2046.0+4954 (G)	C	19(S)	0.8(S)	90'- 120'	0.007 0.01 0.013 (F)	Y	17
27	G114. 3+0.3	23h 37m 00s	61° 55' 00"	Y	2FGL J2333.3+6237 (G)	S	4.1(S)	0.7(S)	55'- 90'	0.006(F)	Y	17
28	G116. 5+1.1	23h 53m 40s	63° 15' 00"	Y	2FGL J2358.9+6325 (G)	S	280(S)	1.6(S)	60' - 80'	0.005(F)		17
29	G132. 7+1.3 (HB3)	02h 17m 40s	62° 45' 00"	Y	2FGL J0214.5+6251 c,J0218.7+620 8c,J0221.4+62 57c(G)	S		2.2(S)	80'	0.006 0.013 0.016 (F)	Y?	17
30	G140. 25-16. 75	02h 23m 12s	43° 00' 42"	Y	MAGIC J0223+403(T)					0.022(≥0 .15TeV)(MA		111
31	G160. 9+2.6 (HB9)	05h 01m 00s	46° 40' 00"	Y	2FGL J0503.2+4643 (G)	C		1.5-4(S)	120'- 140'	0.006(F)	Y?	17
32	G166. 0+4.3 (VRO 42.05. 01)	05h 26m 30s	42° 56' 00"	Y	2FGL J0526.6+4308 (G)	S		4.5(S)	35'-5 5'	0.004(F)	Y?	17
33	G179. 0+2.6	05h 53m 40s	31° 05' 00"	Y	2FGL J0553.9+3104 (G)	S?			70'	0.014(F)		17

34	G180. 0-1.7(S147)	05h 39m 00s	27° 50' 00"	Y	2FGL J0538.1+2718 (G)	S PWN	26-34 (S),6 20(P)	0.36-0.88 (S),1.47(P)	180'	0.007(F)		17
35	G201. 3+0.5 1	06h 31m 49.22s	10° 34' 12.7"	Y	0FGL J0631.8+1034	PWN		6.55(P)		0.29(Mi)		
36	G260. 4-3.4(Puppi s A)	08h 22m 10s	-43° 00' 00"	Y	2FGL J0821.0-4254, J0823.0-4246, J0823.4-4305	S	3.4(S)	2.2	50'-6 0'	0.008 0.031 0.007 (F)		17, 112
37	G284. 8-0.52	10h 26m 38.4s	-58° 12' 00"	N	HESS J1026-582(T)	PWN				0.032(\geq 0 .8TeV)(H)		113
38	G287. 4+0.6 (Pupp y)	10h 48m 16.7s	-58° 31' 48"	N	2FGL J1048.2-5831(G)	C? PWN		3(P)		0.154(F)		
39	G291. 0-0.1(MSH 11-62)	11h 11m 54s	-60° 38' 00"	N	2FGL J1112.1-6040 (G)	C PWN	1.3-1 0(S)	1-11(S)	13'-1 5'	0.069(F)		17
40	G298. 6-0.0	12h 13m 41s	-62° 37' 00"	N	2FGL J1214.0-6237(G)	S			9' - 12'	0.038(F)		17
41	G304. 6+0.1 (Kes 17)	13h 05m 59s	-62° 42' 00"	N	(G)	S		9.7(S)	8'	?(F)	Y	114
42	G314. 41-0.1 4	14h 27m 52s	-60° 51' 00"	N	HESS J1427-608(T)					0.05(0.97 -50TeV)(H)		79, 80
43	G315. 1+2.7	14h 24m 30s	-57° 50' 00"	N	2FGL J1411.9-5744(G)	S			150'- 190'	0.007(F)		17
44	G316. 3-0.0(MSH 14-57)	14h 41m 30s	-60° 00' 00"	N	2FGL J1441.6 -5956(G)	S		\geq 7.2(S)	14'- 29'	0.02(F)		17
45	G317. 95-3.4 9	15h 06m 52.8s	-62° 21' 00"	N	HESS J1507-622(T)	PWN ?	1?			0.01(\geq 1T eV)(H)		79, 80, 115

46	G319. 62+0. 29	15h 03m 38s	-58h 13m 45s	N	HESS J1503-582(T)					0.06(≥ 1 T eV)(H)		
47	G321. 9-0.3	15h 20m 40s	-57° 34' 00"	N	2FGL J1521.8-5735 (G)	S			23'- 31'	0.049(F)		17
48	G326. 3-1.8(MSH 15-56)	15h 53m 00s	-56° 10' 00"	N	2FGL J1552.8-5609(G)	C PWN		≥ 1.5 (S)	38'	0.027(F)		17
49	G332. 4+0.1 (Kes 32, MSH 16-51)	16h 15m 20s	-50° 42' 00"	N	2FGL J1615.0-5051(G)	S	0.3-3 (S)	7-11(S)	15'	0.066(F)		17
50	G336. 38+0. 19	16h 32m 09.6s	-47° 49' 12"	N	HESS J1632-478(T)	PWN				0.12($\geq 0.$ 2TeV)(H)		
51	G336. 7+0.5	16h 32m 11s	-47° 19' 00"	N	2FGL J1631.7-4720c	S			10'- 14'	0.034(F)		17
52	G343. 0-6.0(RCW 114)	17h 25m 00s	-46° 30' 00"	N	2FGL J1727.3-4611(G)	S			250'	0.005(F)		17
53	G343. 10-2.6 8?	17h 09m 42.2s	-44° 28' 57"	N	PSR B1706-44(T?)			2.5		≤ 0.02 (≥ 0 .5TeV)(H ,C)		
54	G350. 1-0.3	17h 17m 40s	-37° 24' 00"	N	2FGL J1718.1-3725(G)	S?	0.9(S)	4.5(S)	4'	0.018(F)		17, 116
55	G353. 44-0.1 3	17h 29m 35s	-34° 32' 22"	N	HESS J1729-345(T)					?(H)		100
56	G355. 4+0.7	17h 31m 20s	-32° 26' 00"	N	2FGL J1731.6-3234c (G)	S			25'	0.027(F)		17
57	G356. 3-0.3	17h 37m 56s	-32° 16' 00"	N	2FGL J1737.2-3213(G)	S			7'- 11'	0.031(F)		17
58	G357. 7-0.1(17h 40m 29s	-30° 58' 00"	N	2FGL J1740.4-3054	S?		11.8(S)	3'- 8'	0.052(F)	Y	17

	The Tornado, MSH 17-39)				c(G)							
59	G358.4+0.19	17h 41m 00s	-30° 12' 00"	N	HESS J1741-302(T)					0.01(\geq 1TeV)(H)		
60	G358.5-0.9	17h 46m 10s	-30° 40' 00"	N	2FGL J1745.5-3028 c(G)	S			17'	0.023(F)		17
61	G359.1+0.9	17h 39m 36s	-29° 11' 00"	N	2FGL J1738.9-2908 (G)	S			11'-12'	0.037(F)		17

Table 2 has the same caption as Table 1.

3. The Prospect of CR originating from SNRs

Next generation very-high-energy telescope arrays will detect more Galactic TeV gamma-ray sources. E.g. LHAASO (see other papers on LHAASO in the special supplement).

It will be expected to identify more faint SNR / TeV γ -ray source associations by employing new generational multi-waveband survey data (e.g., radio survey from the new Australian Square Kilometer Array (ASKAP) telescope) so that we may test these ideas to solve the CR origin puzzle. We have been involved in next generation radio telescope survey programs, e.g. The Galactic Australian Square Kilometer Array Pathfinder survey (GASKAP, also see link for the detail: <http://www.astro.keele.ac.uk/~jacco/research/GASKAP.pdf>). GASKAP is a survey of emission and absorption at 21 cm (the HI line) and of maser emission, diffuse emission, etc. It is an order of magnitude deeper than any survey at comparable resolution (e.g. International Galactic Plane Survey (composed of VLA Galactic Plane Survey (VGPS), CGPS and SGPS, one of the excellent surveys currently available. See Fig. 2). It covers an order of magnitude more area at low latitudes than any survey at comparable sensitivity (e.g. The Galactic Arecibo L-Band Feed Array HI Survey (GALFA), see Fig. 3).

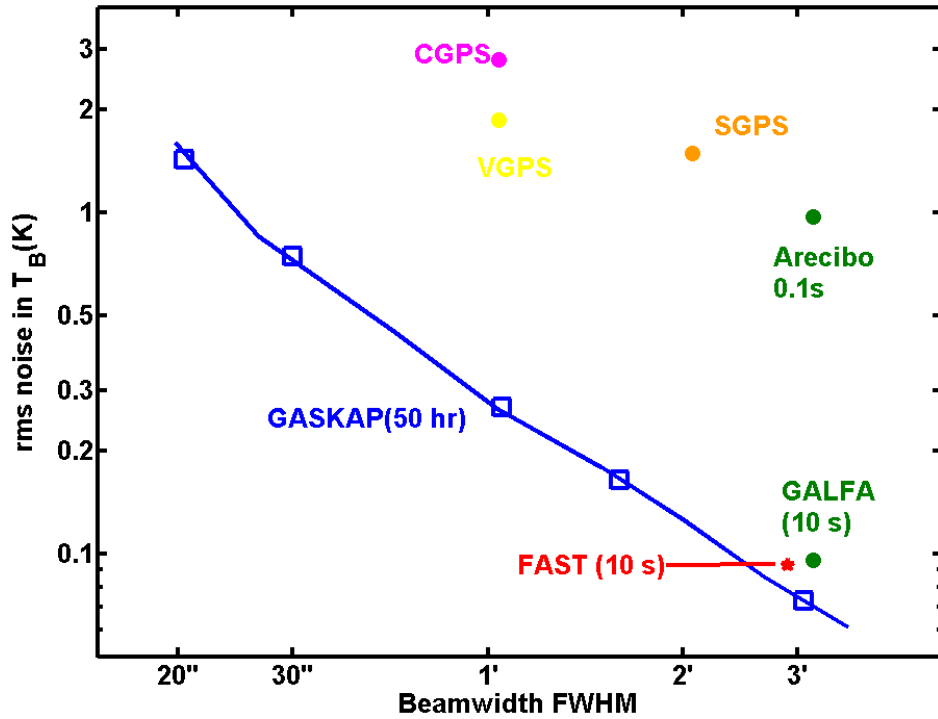


Fig. 2. (Color online) The GASKAP brightness sensitivity vs. resolution (beamwidth), for the medium integration time of 50 hours, with spectra smoothed to 1 km/s. The other two survey speeds give sensitivities a factor of two higher or lower. H I emission mapping at low latitudes will make use of resolution from 20'' to 1'', depending on the brightness and angular scales of the emission in each field. FAST is the Chinese next general 500 m single-dish radio telescope. We obtain this Figure by editing Figure 5 in our GASKAP proposal.

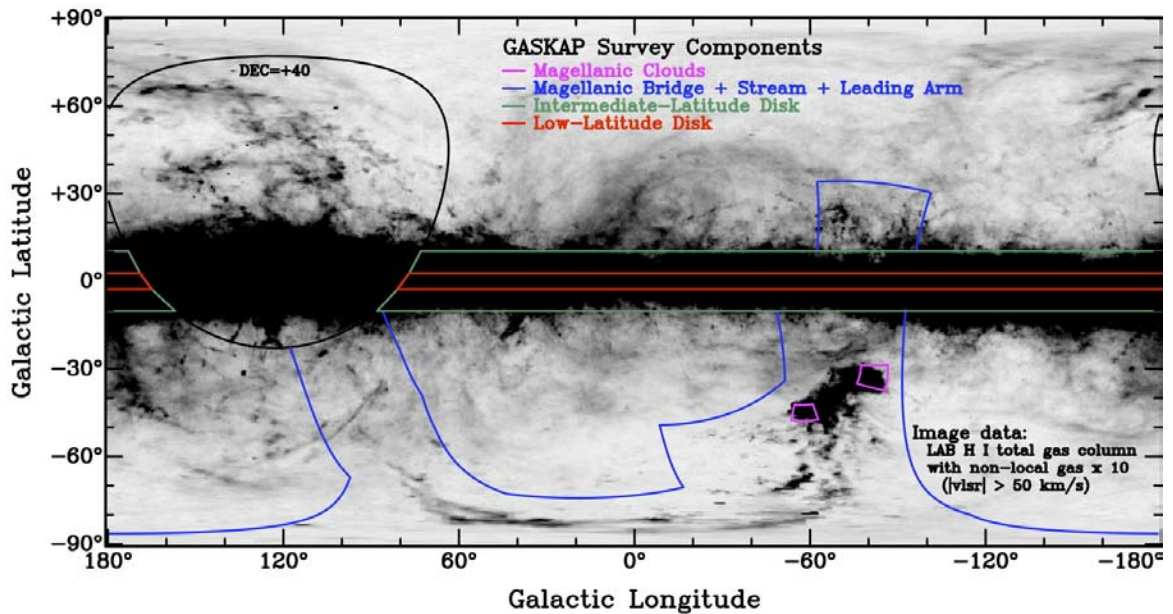


Fig. 3. (Color online) The GASKAP survey areas in Galactic coordinates, with H I column densities (grey scale) in the background. The region north of DEC = +40 Degree must be filled in

from the Northern Hemisphere. Fig. 3 is from Fig. 4 of our GASKAP proposal.

ASKAP will start to run in 2013. We expect that we should detect many faint Galactic SNRs by employing ASKAP. We had previously developed distance-determination methods by giving results from HI and CO line spectra of some SNRs[117,118], so we can use GASKAP data to determine distances to the faint SNRs associated with TeV sources in order to obtain their basic parameters such as the luminosity and age. By combining the deeper very-high-energy-telescopes surveys, we believe that our research may advance understanding of the CRs' origin.

We acknowledge supports from the NSFC program (011241001, 11261140641). This publication was made possible through the support of a grant from the John Templeton Foundation and National Astronomical Observatories (NAO) of the CAS. The opinions expressed in this publication are those of the authors and do not necessarily reflect the views of the John Templeton Foundation or NAOCAS. The funds from John Templeton Foundation were grant from the University of Chicago which also manages the program in conjunction with NAO CAS.

References

- 1 Blandford R, Eichler D. Particle acceleration at astrophysical shocks: A theory of cosmic ray origin. *Phys Rep*, 1987, 154, 1
- 2 Aharonian F, Akhperjanian A G, Bazer-Bachi A.R. et al. The H.E.S.S. Survey of the Inner Galaxy in Very High Energy Gamma Rays. *Astrophys J*, 2006, 636, 777
- 3 Uchiyama Y, Aharonian F A, Tanaka T et al. Extremely fast acceleration of cosmic rays in a supernova remnant. *Nature*, 2007, 449, 576
- 4 Yamazaki R, Kohri K, Bamba A et al. TeV γ -rays from old supernova remnants. *Mon Not R Astron Soc*, 2006, 371, 1975
- 5 Ioka K, Mészáros P. Hypernova and Gamma-ray Burst Remnants as TeV Unidentified Sources. *Astrophys J*, 2010, 709, 1337
- 6 Butt Y M, Schneider N, Dame T M et al. The Molecular Environment of the Gamma-Ray Source TeV J2032+4130. *Astrophys J*, 2008, 676, 123
- 7 Enomoto R, Tanimori T, Naito T et al. The acceleration of cosmic-ray protons in the supernova remnant RX J1713.7-3946. *Nature*, 2002, 416, 823
- 8 Tian W W, Li Z, Leahy D A et al. X-Ray Emission from HESS J1731-347/SNR G353.6-0.7 and Central Compact Source XMMS J173203-344518. *Astrophys J*, 2010, 712, 790
- 9 Tian W W, Li Z, Leahy D A, Wang Q D. VLA and XMM-Newton Observations of the SNR W41/TeV Gamma-Ray Source HESS J1834-087. *Astrophys J*, 2007, 657, L25
- 10 Tian W W, Leahy D A, Haverkorn M et al. Discovery of the Radio and X-Ray Counterpart of TeV γ -Ray Source HESS J1731-347. *Astrophys J*, 2008, 679, L85
- 11 Green D A. A revised Galactic supernova remnant catalogue. *Bull. Astron. Soc. India*, 2009, 37, 45
- 12 Brogan C L, Gelfand J D, Gaensler B M et al. Discovery of 35 New Supernova Remnants in the Inner Galaxy. *Astrophys J*, 2006, 639, 25
- 13 Kothes R, Uyaniker B, Reid R I. Two new Perseus arm supernova remnants discovered in the Canadian Galactic Plane Survey. *Astron Astrophys*, 2005, 444, 871

- 14 Tian W W, Leahy D A, Foster T J Discovery of a new faint radio SNR G108.2-0.6. *Astron Astrophys*, 2007,465, 907
- 15 Gao X Y, Sun X H, Han J L et al. A Sino-German $\lambda 6$ cm polarization survey of the Galactic plane. VI. Discovery of supernova remnants G178.2-4.2 and G25.1-2.3. *Astron Astrophys*, 2011,532, 144
- 16 Ferrand G, Safi-Harb S. A Census of High-Energy Observations of Galactic Supernova Remnants. *Adv Space Res*, 2011,49:1313-1319
- 17 Abdo A A, Ackermann M, Ajello M et. al. [Fermi Collaboration] ‘Fermi Large Area Telescope Second Source Catalog’. *Astrophys J Supp*, 2012, 199 31
- 18 Vlasios V, James C, Nicola O et. al. ‘Fermi LAT detection of an outburst from the Galactic center region’. *The Astronomer's Telegram*, 2011, 3162
- 19 Trap G, Goldwurm A, Dodds-Eden K et. al. Concurrent X-ray, near-infrared, sub-millimeter, and GeV gamma-ray observations of Sagittarius A*. *Astron Astrophys*, 2011, 528, A140
- 20 Abramowski A, Acero F, Aharonian F et. Al. [H.E.S.S. Collaboration]. Search for a Dark Matter Annihilation Signal from the Galactic Center Halo with H.E.S.S.. *Phys Rev Lett* 2011, 106, 161301
- 21 Roland M C. Galactic centre star formation writ large in gamma-rays. *arXiv:1103.4523v2*
- 22 van Eldik C et. al. [H. E. S. S. Collaboration]. The Very High Energy γ -ray View of the Galactic Centre as of Early 2010. *arXiv:1105.3596*
- 23 Michael J L. Time Variation of GeV Gammas from the Galactic Center with a Period ~ 4 yr. *arXiv:1109.6280*
- 24 Beilicke M et. al. [the VERITAS Collaboration]. The Galactic Center Region Imaged by VERITAS. *arXiv:1109.6836*
- 25 Dan H, Tim L. Origin of the gamma rays from the Galactic Center. *Phys Rev D*, 2011, 84, 123005
- 26 Viana A. The galactic center region viewed by H.E.S.S.. *arXiv:1111.5783*
- 27 Jones D I, Burton M, Jones P et. al. The Milky Way Heart: Investigating molecular gas and gamma-ray morphologies in the Central Molecular Zone. *arXiv:1104.0161*
- 28 Holler M, Schöck F M, Eger P et. al. Spatially resolved X-ray spectroscopy and modeling of the nonthermal emission of the PWN in G0.9+0.1. *Astron Astrophys*, 2011,539, A24
- 29 Makoto S, Katsuji K. X-Ray Observations of the Supernova Remnant W28 with Suzaku --- I. Spectral Study of the Recombining Plasma. *Publ Astron Soc Japan*, 2012, Vol.64 No. 4
- 30 Ajello M, Allafort A, Baldini L et. al. Fermi Large Area Telescope Observations of the Supernova Remnant G8.7-0.1. *Astrophys J*, 2012, 744 80
- 31 Hofverberg P, Chaves R C G, Méhault J et. al. Discovery of VHE gamma-ray emission from the SNR G15.4+0.1 with H.E.S.S. *arXiv:1112.2901*
- 32 Mayer M, Brucker J, Jung I et. al. Implications on the X-ray emission of evolved pulsar wind nebulae based on VHE gamma-ray observations. *arXiv:1202.1455v2*
- 33 Grondin M H, Funk S, Lemoine-Goumard M et. al. Detection of the Pulsar Wind Nebula HESS J1825-137 with the Fermi Large Area Telescope. *Astrophys J*, 2011, 738 42
- 34 Adam V E, Roger W R. Multi-Zone Modeling of HESS J1825-137. *Astrophys J*,

- 2011,742 62
- 35 Ackermann M, Ajello M, Baldini L et. al. Fermi-LAT Search for Pulsar Wind Nebulae Around Gamma-ray Pulsars. *Astrophys J*, 2011, 726 35
 - 36 Laffon H, Khélifi B, Brun F et. al. Evidence for VHE emission from SNR G22.7-0.2 region with H.E.S.S. arXiv:1110.6890
 - 37 Li H, Chen Y. Gamma-rays from molecular clouds illuminated by accumulated diffusive protons. II: interacting supernova remnants. *Mon Not R Astron Soc*, 2012, 421: 935-942
 - 38 Misanovic Z, Kargaltsev O, Pavlov G G. Chandra Observation of the TeV Source HESS J1834-087. *Astrophys J*, 2011, 735 33
 - 39 Temim T, Slane P, Arendt R G. Infrared and X-Ray Spectroscopy of the Kes 75 Supernova Remnant Shell: Characterizing the Dust and Gas Properties. *Astrophys J*, 2012, 745 46
 - 40 Zhou P, Chen Y. Molecular Environment and an X-Ray Spectroscopy of Supernova Remnant Kesteven 78. *Astrophys J*, 2012, 743 4
 - 41 <http://www.mpi-hd.mpg.de/hfm/HESS/pages/home/som/2011/02/>
 - 42 Paron S., Giacani E., Rubio M. Study of the molecular clump associated with the high-energy source HESS J1858+020. *Astron Astrophys*, 2011, 530 A25
 - 43 Torres D F, Li H, Chen Y. Cosmic rays in the surroundings of SNR G35.6-0.4. *Mon Not R Astron Soc*, 2011, 417 3072-3079
 - 44 Ackermann M, Ajello M, Baldini L et. al. Fermi-LAT Search for Pulsar Wind Nebulae Around Gamma-ray Pulsars. *Astrophys J*, 2012, 726 35
 - 45 Cao Z, Chen S Z for the ARGO-YBJ collaboration. TeV gamma-ray survey of the northern sky using the ARGO-YBJ experiment. arXiv:1110.1809
 - 46 Zhou X, Miceli M, Bocchino F. Unveiling the spatial structure of the overionized plasma in the supernova remnant W49B. *Mon Not R Astron Soc*, 2011, 415 244-250
 - 47 Brun F, de Naurois M, Hofmann W, et. al. Discovery of VHE gamma-ray emission from the W49 region with H.E.S.S. arXiv:1104.5003
 - 48 Aleksić J, Alvarez EA, Antonelli LA et. al. [MAGIC Collaboration] Morphological and spectral properties of the W51 region measured with the MAGIC telescopes. *Astron Astrophys*, 2011, 541 A13
 - 49 Tibolla O for the MAGIC collaboration. Recent Results from the MAGIC Telescopes. arXiv:1201.2295
 - 50 Krause J, Carmona E, Reichardt I for the MAGIC Collaboration. Probing proton acceleration in W51C with MAGIC. arXiv:1111.0066
 - 51 Carmona E, Krause J, Reichardt I. Probing proton acceleration in W51C with MAGIC. arXiv:1110.0950
 - 52 Bartoli B, Bernardini P, Bi X J.et. al. Observation of TeV Gamma Rays from the Cygnus Region with the ARGO-YBJ Experiment. *Astrophys J*, 2012, 745 L22
 - 53 Aliu E for the VERITAS Collaboration. Observations of SNR CTA 1 and the Cyg OB1 region with VERITAS. arXiv:1110.4656
 - 54 Safi-Harb S, Matheson H, Kothes R On the Plerionic Supernova Remnant CTB 87 (G74.9+1.2) and Its Powering Engine: Insights from the Chandra X-ray Observatory. *AAS Meeting,2011, Vol. 43 #218, #228.08*
 - 55 Abdo A A, Allen B T, Aune T et. al. Spectrum and Morphology of the Two Brightest

- Milagro Sources in the Cygnus Region: MGRO J2019+37 and MGRO J2031+41. *Astrophys J*, 2012,753:A159
- 56 Vissani F., Aharonian F. Galactic Sources of High-Energy Neutrinos: Highlights. *Nucl Instr Meth Phys Res A*,2011,692:5-12
 - 57 Amanda W. for the VERITAS Collaboration. Recent Observations of Supernova Remnants with VERITAS. arXiv:1111.2093
 - 58 Amanda W. for the VERITAS Collaboration. Detection of VER J2019+407 (G78.2+2.1) and Tycho's Supernova Remnant with VERITAS. arXiv:1111.1034
 - 59 Ackermann M., Ajello M., Allafort A. et. al. The cosmic-ray and gas content of the Cygnus region as measured in γ -rays by the Fermi Large Area Telescope. *Astrophys J*, 2012 , 538, A71
 - 60 Tibaldo L, Grenier I A for the Fermi LAT collaboration. The Fermi-LAT view of cosmic rays and interstellar gas in the Cygnus region: a not so special spot of the Local Arm. arXiv:1110.6852
 - 61 Aliu E, Gotthelf E, Wakely S et. al. Multiwavelength Study Of The Large Radio Feature SNR G106.3+2.7 Using SUZAKU, LAT , VERITAS And GBT. AAS, 2011, HEAD meeting #12, #34.23
 - 62 Patnaude D J, Vink J, Laming J M et. al. A Decline in the Nonthermal X-ray Emission from Cassiopeia A. *Astrophys J*, 2011,729, L28
 - 63 McArthur S for the VERITAS Collaboration. VHE Observation of CTA 1 with VERITAS arXiv:1111.2591
 - 64 Abdo A A, Wood K S, DeCesar M E et. al. PSR J0007+7303 in the CTA1 Supernova Remnant: New Gamma-Ray Results from Two Years of Fermi Large Area Telescope Observations. *Astrophys J*, 2012, 744 146
 - 65 Tian W W, Leahy D A. Tycho SN 1572: A Naked Ia Supernova Remnant Without an Associated Ambient Molecular Cloud. *Astrophys J*, 2011, 729 L15
 - 66 Acciari V A, Aliu E, Arlen T et. al. Discovery of TeV Gamma-ray Emission from Tycho's Supernova Remnant. *Astrophys J*, 2011,730 L20
 - 67 Giordano F, Naumann-Godo M, Ballet J. Fermi Large Area Telescope Detection of the Young Supernova Remnant Tycho. *Astrophys J*, 2012, 744 L2
 - 68 Atoyan A, Dermer C Gamma Rays from the Tycho Supernova Remnant: Leptonic or Hadronic? arXiv:1111.4175
 - 69 Edmon P P, Kang H, Jones T W et. al. Non-thermal radiation from Type Ia supernova remnants. *Mon Not R Astron Soc*, 2011, 414:3521-3536
 - 70 Eriksen K A, Hughes J P, Badenes C et. al. Evidence for Particle Acceleration to the Knee of the Cosmic Ray Spectrum in Tycho's Supernova Remnant. *Astrophys J*,2011, 728 L28
 - 71 Abdo A A, Allen B T, Aune T et. al. Observation and Spectral Measurements of the Crab Nebula with Milagro. *Astrophys J*, 2012, 750 63
 - 72 Loparco F[Fermi LAT Collaboration] Spectral analysis of the Crab Pulsar and Nebula with the Fermi Large Area Telescope. *Nucl Instr Meth Phys Res A*,2011, 630 136
 - 73 Kohri K, Ohira Y, Ioka K. Gamma-ray flare and absorption in Crab Nebula: Lovely TeV--PeV astrophysics. *Mon Not R Astron Soc*, 2012, 424 :2249-2254
 - 74 Giordano F[Fermi-LAT collaboration] Study of the IC443 SNR with the Fermi LAT. *Nucl*

- Instr Meth Phys Res Section A, 2011, 630 163
- 75 Mattana F, Götz D, Terrier R et. al. Extended Hard X-Ray Emission from the Vela Pulsar Wind Nebula. *Astrophys J*, 2011, 743 L18
 - 76 Tanaka T, Allafort A, Ballet J et. al. Gamma-Ray Observations of the Supernova Remnant RX J0852.0-4622 with the Fermi Large Area Telescope. *Astrophys J*, 2011, 740 L51
 - 77 Acero F, Gallant Y, Terrier R et. al. A new nearby PWN overlapping the Vela Jr SNR. *MmSAI*, 2011, 82 752
 - 78 Ackermann M et al. [Fermi Collaboration] Periodic Emission from the Gamma-ray Binary 1FGL J1018.6-5856. *Science*, 2012, 335, 189
 - 79 Tibolla O., Mannheim K., Elsässer D. et. al. Ancient Pulsar Wind Nebulae in light of recent GeV and TeV observations. arXiv:1111.1634
 - 80 Tibolla O, Mannheim K, Kaufmann S et. al. New developments in the ancient Pulsar Wind Nebulae scenario. arXiv:1109.3144
 - 81 Abramowski A et. al. [HESS Collaboration] Discovery of the source HESS J1356-645 associated with the young and energetic PSR J1357-6429. *Astron Astrophys*, 2011, 533 A103
 - 82 Lemoine-Goumard M, Zavlin V E, Grondin MH. Discovery of gamma- and X-ray pulsations from the young and energetic PSR J1357-6429 with Fermi and XMM-Newton. *Astron Astrophys*, 2011, 533 A102
 - 83 Chang C, Pavlov G G, Kargaltsev O. X-Ray Observations of the Young Pulsar J1357—6429 and Its Pulsar Wind Nebula. *Astrophys J*, 2012 744 81
 - 84 Yamaguchi H, Koyama K, Uchida H. Suzaku View of the Supernova Remnant RCW 86: X-Ray Studies of Newly-Discovered Fe-Rich Ejecta. *Publ Astron Soc Japan*, 2011, 63 S837-S848
 - 85 Brian J W., William P B, John M B, RCW 86: A Type Ia Supernova in a Wind-Blown Bubble. *Astrophys J*, 2011 741 96
 - 86 Hofverberg P, Chaves R C G, Fiasson A et. al. Discovery of VHE gamma-rays from the vicinity of the shell-type SNR G318.2+0.1 with H.E.S.S. arXiv:1104.5119
 - 87 Acero F, Djannati-Ataï A, Förster A et. al. Detection of TeV emission from the intriguing composite SNR G327.1-1.1. arXiv:1201.0481
 - 88 Eger P, Rowell G, Kawamura A et. al. A multi-wavelength study of the unidentified TeV gamma-ray source HESS J1626-490. *Astron Astrophys*, 2011, 526 A82
 - 89 Abramowski A et. al. [HESS Collaboration] Detection of very-high-energy γ -ray emission from the vicinity of PSR B1706-44 and G 343.1-2.3 with H.E.S.S. *Astron Astrophys*, 2011, 528 A143
 - 90 Giacani E, Smith M J S, Dubner G et. al. A new study of the supernova remnant G344.7-0.1 located in the vicinity of the unidentified TeV source HESS J1702-420. *Astron Astrophys*, 2011, 531 A138
 - 91 Yamaguchi H, Tanaka M Maeda K et. al. Elemental Abundances in the Possible Type Ia Supernova Remnant G344.7-0.1. *Astrophys J*, 2012 749 137
 - 92 Fujinaga T, Bamba A, Dotani T et. al. Suzaku Observation of the Unidentified Very High Energy Gamma-Ray Source HESS J1702-420. *Publ Astron Soc Japan*, 63 S857-S864
 - 93 Abdo A A, Ackermann M, Ajello M et. al. Observations of the Young Supernova

- Remnant RX J1713.7-3946 with the Fermi Large Area Telescope. *Astrophys J*, 2011, 734 28
- 94 Li H, Liu S M, Chen Y. Derivation of the Electron Distribution in Supernova Remnant RX J1713.7-3946 via a Spectral Inversion Method. *Astrophys J*, 2011, 742 L10
- 95 Ellison Donald C, Slane P, Patnaude Daniel J et. al. Core-collapse Model of Broadband Emission from SNR RX J1713.7-3946 with Thermal X-Rays and Gamma Rays from Escaping Cosmic Rays. *Astrophys J*, 2012, 744 39
- 96 Maxted Nigel I, Rowell Gavin P, Dawson Bruce R et. al. 3 to 12 millimetre studies of dense gas towards the western rim of supernova remnant RX J1713.7-3946. *Mon Not R Astron Soc*, 2230–2245 2012
- 97 Tian W W, Leahy D A. Distances of the TeV supernova remnant complex CTB 37 towards the Galactic bar. *Mon Not R Astron Soc*, 2012, 421 2593–2597
- 98 Sezer A, Gök F, Hudaverdi M et. al. Suzaku observation of the Galactic supernova remnant CTB 37A (G348.5+0.1). *Mon Not R Astron Soc*, 2011, 417 1387-1391
- 99 Horvath J E, Allen M P The supernova remnant CTB 37B and its associated magnetar CXOU J171405.7-381031: evidence for a magnetar-driven remnant. *Res Astron Astrophys*, 2011, 11 625-630
- 100 H.E.S.S. Collaboration. A new SNR with TeV shell-type morphology: HESS J1731-347. *Astron Astrophys*, 2011, 531 A81
- 101 Ohnishi T, Koyama K, Tsuru T G, et. al. X-Ray Spectrum of a Peculiar Supernova Remnant, G359.1-0.5. *Publ Astron Soc Japan*, 2011, 63 527-533
- 102 Hui C Y, Wu E M H, Wu J H K et. al. Exploring the Dark Accelerator HESS J1745-303 with the Fermi Large Area Telescope. *Astrophys J*, 2011, 735 115
- 103 Caprioli D. Understanding hadronic gamma-ray emission from supernova remnant. *J Cosmol Astropart Phys*, 2011, 05, 26
- 104 Jiang B, Chen Y, Wang J Z et. al. Cavity of Molecular Gas Associated with Supernova Remnant 3C 397. *Astrophys J*, 2010, 712, 1147-1156
- 105 Sheidaei F, Djannati-Ataï A, Gast H for the HESS Collaboration. Discovery of very-high-energy gamma-ray emission from the vicinity of PSR J1831-952 with H.E.S.S. arXiv:1110.6837
- 106 Giuliani A., Cardillo M., Tavani M. et. al. Neutral Pion Emission from Accelerated Protons in the Supernova Remnant W44. *Astrophys J*, 2011, 742 L30
- 107 Klepser S, Krause J, Doro M. for the MAGIC collaboration. Mapping the extended TeV source HESS J1857+026 down to Fermi-LAT energies with the MAGIC telescopes. *Astrophys J*, 2012, 748 141
- 108 Wu J H K, Kong A K H, Huang R H H et. al. Discovery of γ -ray pulsation and X-ray emission from the black widow pulsar PSR J2051-0827. arXiv:1201.5980
- 109 Arzoumanian Z, Gotthelf E V, Ransom S M et. al. Discovery of an Energetic Pulsar Associated with SNR G76.9+1.0. *Astrophys J*, 2011, 739 39
- 110 Murakami H, Kitamoto S, Kawachi A et. al. Detection of X-Ray Emission from the Unidentified TeV Gamma-Ray Source TeV J2032+4130. *Publ Astron Soc Japan*, 2011, 63 S873-878
- 111 Sudou H, Iguchi S. Proper Motion of the Sub-parsec Scale Jet in the Radio Galaxy 3C

- 66B. *Astron J*, 2011, 142 49
- 112 De Luca A, Salvetti D, Sartori A et. al. A time-variable, phase-dependent emission line in the X-ray spectrum of the isolated neutron star RX J0822-4300. *MNRAS*, 2012, 421 L72-76
- 113 Abramowski A et. al. [HESS Collaboration] Revisiting the Westerlund 2 field with the HESS telescope array. *Astron Astrophys*, 2011, 525 A46
- 114 Wu J H K, Wu E M H, Hui C Y et. al. Discovery of Gamma-Ray Emission from the Supernova Remnant Kes 17 with Fermi Large Area Telescope. *Astrophys J*, 2011, 740 L12
- 115 Acero F et. al. [HESS Collaboration] Discovery and follow-up studies of the extended, off-plane, VHE gamma-ray source HESS J1507-622. *Astron Astrophys*, 2011, 525 A45
- 116 Lovchinsky I, Slane P, Gaensler B M et. al. A Chandra Observation of Supernova Remnant G350.1-0.3 and Its Central Compact Object. 2011, *Astrophys J*, 731 70
- 117 Tian W W, Leahy D A , Wang Q D. Radio and X-ray images of the SNR G18.8+0.3 interacting with molecular clouds . *Astron Astrophys*, 2007, 474, 541-547
- 118 Tian W W, Leahy D A. The distances of supernova remnants Kes 69 and G21.5-0.9 from HI and 13CO spectra. *Mon Not R Astron Soc*, 2008, 391, L54-58